

# Scintillators

2

## Growth of YAP:Ce and its Application for Secondary Electron Detector for BARC-SEM

S. G. Singh<sup>1\*</sup>, Siddhartha Shankar Pany<sup>2</sup>, G. D. Patra<sup>1</sup>, A. K. Singh<sup>1</sup>, M. Sonawane<sup>1</sup>, Shreyas Pitale<sup>1</sup>, Manoranjan Ghosh<sup>1</sup>, M. Padmanabhan<sup>2</sup>, Shashwati Sen<sup>1</sup> and L. M. Pant<sup>1</sup>

<sup>1</sup>Technical Physics Division, Bhabha Atomic Research Centre (BARC), Trombay – 400085, INDIA

<sup>2</sup>Security Electronics and Cyber Technology Division, Bhabha Atomic Research Centre (BARC), Trombay – 400085, INDIA



BSE detector developed in BARC

### ABSTRACT

Ce doped YAlO<sub>3</sub> (Yttrium Aluminium Pervoskite : YAP) scintillator single crystal of 25 mm dia and 50 mm length has been grown employing Czochralski crystal growth technique. Grown crystal were characterized and processed into detector element for the development of Secondary Electron (SE) and Back-Scattered Electron (BSE) detector for the Scanning electron microscope (SEM) developed at Bhabha Atomic Research Centre. Fabricated SE and BSE detector were tested and qualified for their use in SEM. An ultimate resolution of 20 nm is achieved with SE detectors.

KEYWORDS: Electron Detector, Secondary electron (SE), Scanning electron microscope (SEM)

### Introduction

Ce doped YAlO<sub>3</sub> (YAP:Ce) is one of the excellent scintillators with many advantageous properties like fast decay (~30 ns), good light yield (20-25 k photons/MeV), moderate density (5.3 g/cc) and proportional scintillation response. It is useful in various radiation detection applications like imaging, gamma-ray detectors, timing applications, secondary electron (SE) detector for scanning electron microscope (SEM) and many others [1,2]. Single crystals of YAP are generally grown by the Czochralski technique. The scintillation properties of the materials are highly dependent on the crystal growth parameters [3,4]. In this article we are presenting the growth and scintillation properties of YAP:Ce and development of secondary electron detector.

### Growth and Characterization of YAlO<sub>3</sub>:Ce

Single crystals of YAP:Ce of 60 mm length and 25 mm diameter were grown from the melt using the Czochralski crystal growth technique. Y<sub>2</sub>O<sub>3</sub>, Al<sub>2</sub>O<sub>3</sub> and CeO<sub>2</sub> powders of 99.99% purity were used as starting materials. Powders were mixed in the stoichiometric ratio of 50%Y<sub>2</sub>O<sub>3</sub>-50% Al<sub>2</sub>O<sub>3</sub> (Crystal-I) and 51%Y<sub>2</sub>O<sub>3</sub>-49%Al<sub>2</sub>O<sub>3</sub> (Crystal-II) for the two types of different experiments. The cerium concentration was kept at 0.5 mol% in each experiment. Mixed powders were loaded into an iridium crucible that was placed inside a growth station made from Zirconia based ceramic cylinders. An MF induction heating mechanism based Czochralski crystal puller (Cyberstar, France make Oxypuller) was used to grow the single crystals from the melts. An un-oriented YAP:Ce single crystal of about 6 mm diameter and 40 mm length was used as the seed. A pull rate of about 1 mm/h and a rotation rate of 15 RPM was used in each growth experiment. High pure Ar was used to create inert ambient inside the crystal puller chamber to protect the iridium crucible.

\*Author for Correspondence: S. G. Singh  
E-mail: sgovind@barc.gov.in

After optimization of growth parameters, large size (25 mm diameter and 50 mm length) high quality transparent single crystals of YAlO<sub>3</sub>:Ce were grown successfully. A photograph of an as-grown crystal is shown in Fig.1. Grown crystals were free from any visible defects like inclusion, bubbles etc. Single phase formation was confirmed from the powder X-ray diffraction pattern (not shown in the manuscript).

For scintillation characterization 10x10x10 mm<sup>3</sup> samples were cut from the crystal ingots as shown in Fig.2. Radio-luminescence of the samples was recorded using a white X-ray source (Cu-target) operating at 40 kV - 30 mA and a mono-chromator. All the experiments were carried in 45 degree reflection geometry. The recorded photoluminescence spectra are shown in Fig.3 and are not corrected for the instrument response. It shows the characteristic spin allowed transition of Ce<sup>3+</sup> centre in YAP. The luminescence spectra exhibited the characteristic Ce<sup>3+</sup> emission (370 nm) corresponding to 5d→4f transition [2]. The radio-luminescence spectra for both types of



Fig.1: Single crystal ingot of YAP:Ce.

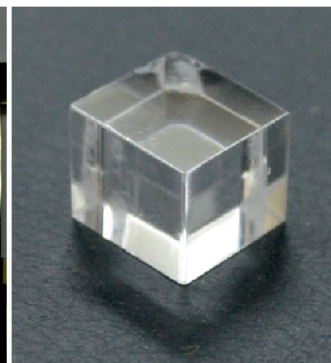


Fig.2: Single crystal sample cut from ingot and processed for characterization.

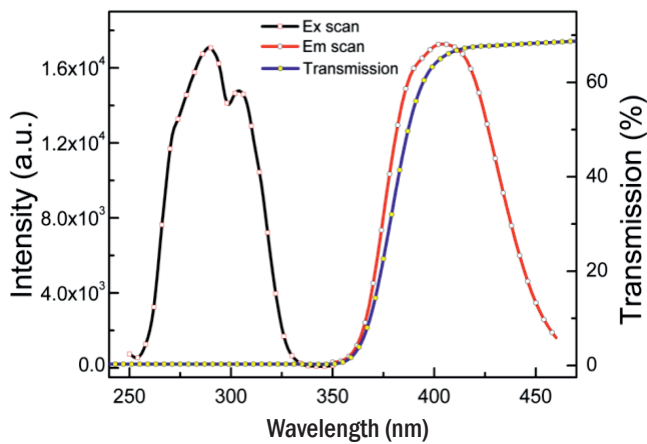


Fig.3: Photo-luminescence and transmission spectra of YAP single crystals.

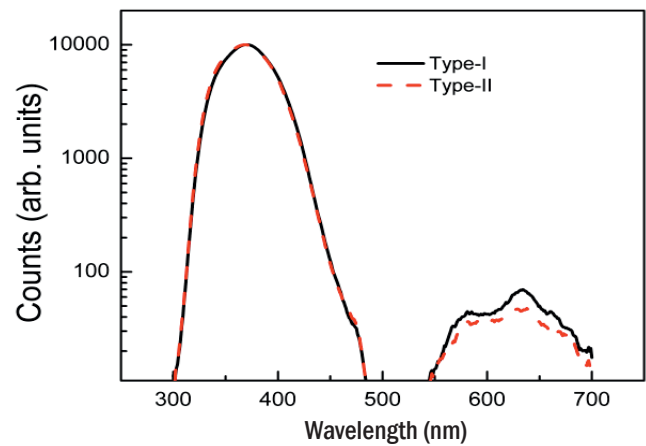


Fig.4: Radio-luminescence spectra of YAP single crystals.

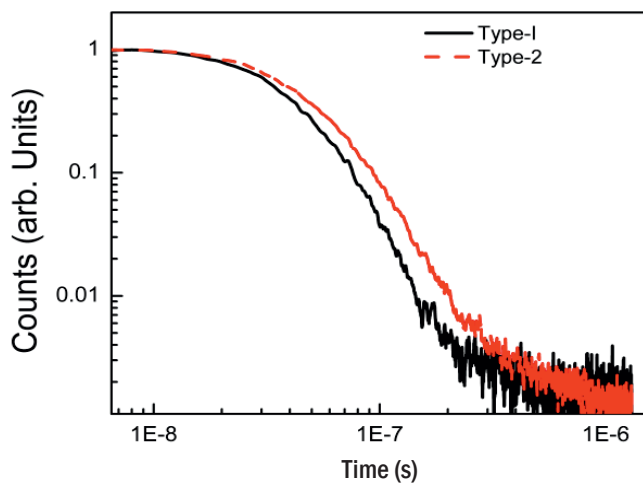


Fig.5: Decay profile of type-I and type-II crystals (for gamma excitation).

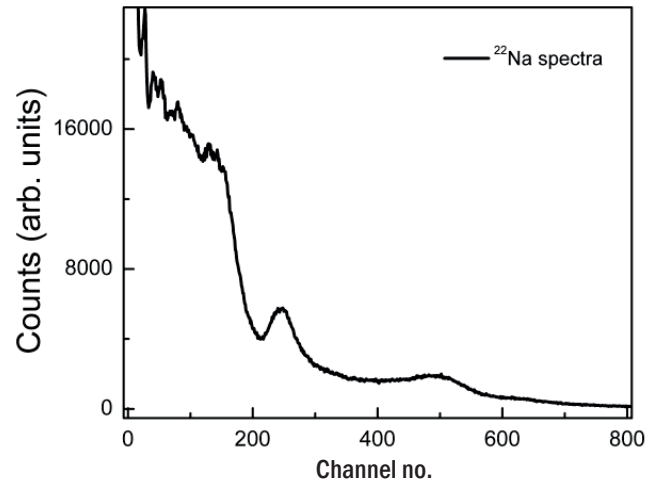


Fig.6: Pulse height spectra of  $^{22}\text{Na}$  recorded using a  $10\times 10\times 10\text{ mm}^3$  YAP:Ce.

crystals are shown in Fig.4. In RL, an emission at longer wavelength (600 nm) accompanied the Ce characteristic emission in both types of crystals. Though the 370 nm emission remains insensitive to the stoichiometric variation in the melt, the contribution of longer wavelength emission is relatively less in type-II crystals. That may be because of less number of  $\text{Y}^{3+}$  related defects in the type-II crystals.

For pulse height and decay time measurements, one face of the cube was polished to optical finish and on remaining faces 5-6 layers of Teflon tape were wrapped. The polished face was then coupled to a PMT (R6095) using silicone based optical grease. An AMPTEK-DP5G MCA was used to record the pulse height spectra ( $^{22}\text{Na}$  source) while a TEKTRONIX (MDO3102) digital storage oscilloscope was used to record decay profile. The recorded decay profiles (for gamma excitation) of the type-I and type-II crystals are shown in Fig.5. It may be seen that the decay profile of type-I crystal is faster ( $\sim 30$  ns) than that of type-II crystal ( $\sim 38$  ns). This difference in the decay profile may be explained on the basis of different kinds of traps in the two types of crystals which are also observed in the RL spectra. The pulse height spectra (Fig.6) of both types of crystals were almost identical and is comparable with reported spectrum for YAP:Ce [1]. The energy resolution measured for the  $^{22}\text{Na}$  gamma source was  $\sim 7\%$  at 511 keV. From these results it is concluded that the stoichiometric variations in the melt considerably affect the timing and other scintillation properties of Ce doped YAP crystal scintillator and crystals grown from stoichiometric ratio of  $\text{Al}_2\text{O}_3:\text{Y}_2\text{O}_3$  yields

better result. For further application only crystals grown from stoichiometric charge (type I) were considered.

### Development of Detectors for Indigenous SEM

#### SE detector

Secondary Electron (SE) detector is a fundamental part to any general-purpose SEM, as it facilitates imaging of the specimen's topographic features. Secondary electrons (SE) ( $\sim 1\text{-}50\text{ eV}$  with mean energy  $\sim 5\text{ eV}$ ) are generated through primary electron beam interaction with specimen. The detection of SE involves acceleration of the SE's to a voltage around 10 keV and using scintillators as detecting element for these accelerated electrons.

The SE detector for BARC-SEM has been designed on this principle that is primarily based on Everheart-Thonley (ET) detector (Fig.7). The detector comprises of 10 mm diameter, 1 mm thick YAP:Ce scintillator single crystal maintained at a voltage of +10 kV to accelerate the secondary electrons. The scintillator is interfaced with fused silica light-guide which is connected to a PMT on the other end. The attractor electrode is maintained at a voltage ranging between +1 kV to -1 kV. While the purpose of the attractor electrode for most SE detectors is to attract the low energy SE towards the detector, the purpose of this electrode in the current design is to focus the stray SE towards the scintillator. In this detector configuration, the electric field generated by scintillator potential directly exerts attracting force on SE.

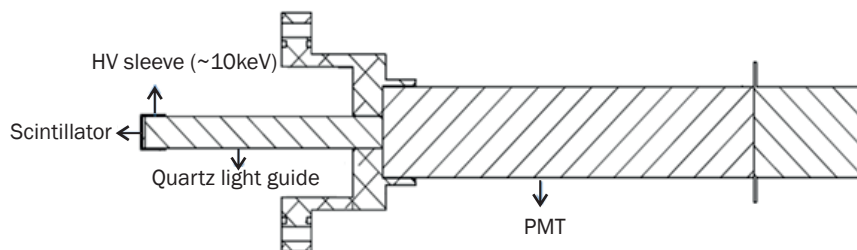


Fig.7: Schematic of ET design based SE detector for BARC-SEM.

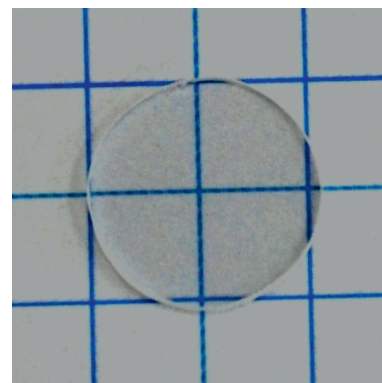


Fig.8: Processed YAP:Ce scintillator (10 mm dia, 1 mm thickness).

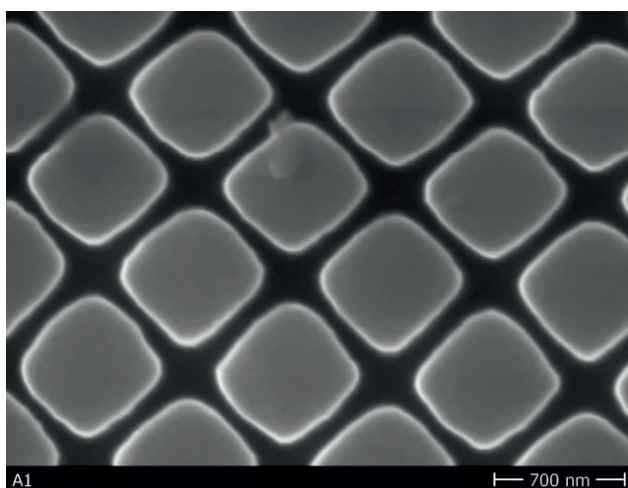


Fig.9: Magnification:1,00,000x, Specimen: SEM Calibration Sample (Recorded employing developed SE detector).

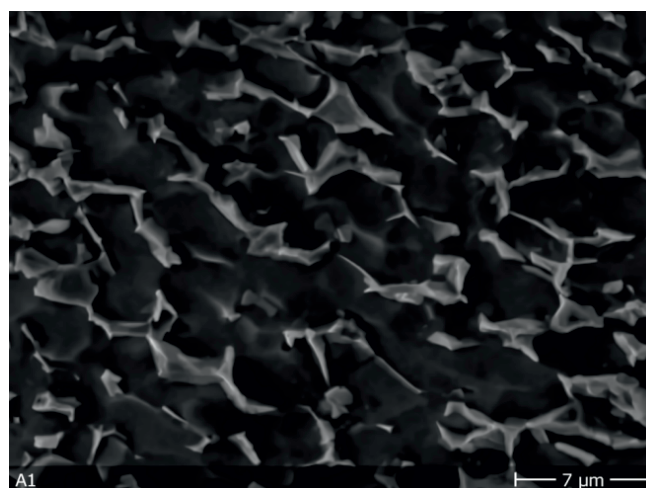


Fig.10: Magnification:10,000x, Specimen: Zr - 2.5% Nb (Recorded employing developed SE detector).

The choice of YAP:Ce as scintillator for SEM detectors is based on its resilience to electron-beam impact, fast decay constant of ~ 30 ns, low after-glow and relatively good photon yield. Single-crystal YAP:Ce scintillators for the detectors have been grown in house using Czochralski crystal growth technique as discussed in the above section. The crystal in the form of ingot of dia. 25 mm and 50 mm length has been processed into scintillators of suitable diameters and 1mm thickness Fig.8. The scintillator disc was polished to optical finish. To prevent electron impact induced charge accumulation on scintillators a 50 nm thick Aluminium layer is deposited on the scintillator crystal outer surfaces using thermal evaporation system. The aluminium layer also functions as a specular reflector for back-propagating scintillation light-rays, and thus enhancing the light collection at PMT. The detector was tested for its performance by incorporating it in a SEM machine and typical images at higher magnification are shown in Fig.9 and 10.

**BSE detector**

The BSE detector is an annular thin plate detector that is placed near the bottom plane of the objective lens. The incident electrons pass through the centre hole of the detector and fall on the sample. Interaction of electron beam with a sample target produces a variety of elastic and inelastic collisions between electrons and atoms within the sample. Elastic scattering depends on atomic number of atoms, consequently, the number of backscattered electrons (BSE) reaching a BSE detector is proportional to the mean atomic number of the sample. Thus, BSE images are very helpful for

obtaining high-resolution compositional maps of a sample and for quickly distinguishing different phases. The BSE detector is similar to the E-T detector. These consist of an Al coated scintillator coupled to a photomultiplier by a light guide. Scintillator based BSE detector can be used down to primary beam energy upto 1.5 keV.

BSE detector designed for BARC-SEM consists of an annular scintillator YAP:Ce crystal of OD 25 mm, ID 6 mm and thickness 1mm. The scintillator is mounted onto a specially designed quartz light-guide, which interfaces with a PMT on the other end (Fig.11). The BSE detector has been designed to double-up as SE detector also, upon application of a positive potential of +10 kV to the scintillator. For fabrication of the detector a disc of 25 mm dia and 2 mm thickness was cut from crystal ingot and processed in to optical finish. An annular hole was cut at the center of the scintillator disc for primary electron beam to pass. The whole assembly was tested for its performance by recording the BSE image shown in Fig.12.

**Conclusion**

The process for growth of YAP:Ce single crystal is developed. The grown crystals were characterized for their performance and were suitable for scintillator applications like x-ray detection and application in SE detectors etc. The crystal was further processed for development of SE detector for BARC-SEM being developed at SESSD. The full process starting from crystal cutting, lapping and polishing to design and fabrication of whole detector assembly was carried and performance of the detector tested in SEM that achieved an ultimate resolution of 20 nm.



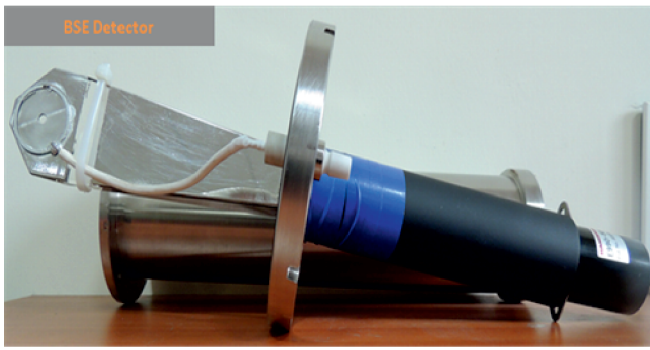


Fig.11: Developed BSE detector.

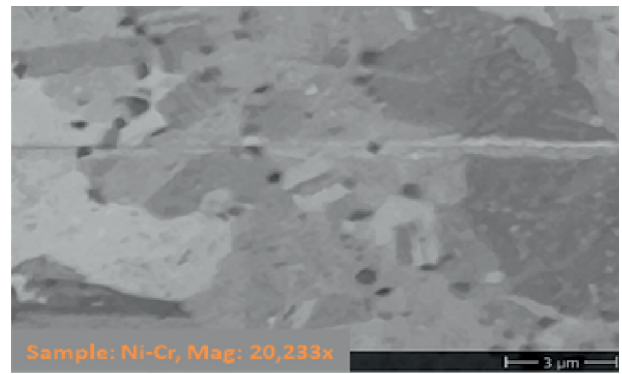


Fig.12: BSE Image of sample Ni-Cr alloy at mag: 22,000.

## References

- [1] Alshourbagy, et al. J. Crystal Growth 303 (2007) 500–505.
- [2] R. Pani, F. de Notaristefani, K. Blazek, P. Maly, R. Pellegrini, A. Pergola, A. Soluri, F. Scopinaro, Nucl. Instr. and Meth. A, 348 (1994) 551.
- [3] B.G. Baryshevsky, et al. J. Phys.: Condens. Matter 5 (1993) 7893-7902.
- [4] M. Moszyński, M. Kapusta, D. Wolski, W. Klamra, B. Cederwall, Nucl. Instr. and Meth. A, 404 (1998) 157.